Green Chemistry

PAPER

View Article Online
View Journal | View Issue

Cite this: *Green Chem.*, 2026, **28**, 6275

A two-step high-throughput screening platform for engineering enzymes to cure unsaturated polyester resins

Christoph Janknecht, [a] Francisca Contreras, [a] Thomke Belthle, [a] Maximilian Nöth, [a] Lukas Kalinka,[a] Tina Radespiel[b] and Ulrich Schwaneberg *[a]

Received 5th December 2025,
Accepted 9th March 2026

DOI: 10.1039/d5gc06576c

rsc.li/greenchem

Unsaturated polyester resins are conventionally cured using cobalt accelerators, which have recently been classified as potentially carcinogenic. Peroxygenase-based enzymatic systems offer a sustainable accelerator alternative if re-engineered to function efficiently under polymerisation conditions in organic solvents. In this work, we present a two-step high-throughput screening platform designed to evolve the peroxygenase's tolerance to organic solvents, followed by the evaluation of the curing performance in polyester resins under application-relevant conditions. Curing was monitored by measuring the consumption of styrene monomer during cross-linking using a 96-well plate Raman spectrometer. The two-step screening platform was validated by screening three site-saturation mutagenesis libraries at positions L61, F157, and L209, located in the substrate tunnel of the unspecific peroxygenase *Hsp*UPO. The variant F157L exhibited a 2.5-fold improvement in tolerance to the organic cosolvent dimethyl sulfoxide (increased residual activity from 26.2 to 66.1% in 67 vol% DMSO) and a 1.2-fold improvement in curing performance (increased conversion rate from 8.22 to 10.14% h^{-1}). The screening platform and obtained results demonstrate that *Hsp*UPO is a promising alternative to toxic cobalt accelerators.

Green foundation

1. Cobalt salts, as the conventional accelerators used in curing unsaturated polyester resins, are now classified as potentially carcinogenic. Engineering peroxygenases to operate under curing conditions offers a safer and sustainable alternative, reducing reliance on hazardous cobalt-based systems.
2. This work introduces a two-step high-throughput screening platform that combines solvent-tolerance enzyme evolution with direct curing-performance assessment in real resin formulations. Using this platform, we identified an unspecific peroxygenase variant (*Hsp*UPO F157L) with increased solvent tolerance and curing performance, demonstrating the feasibility of enzymatic curing in industrially relevant conditions.
3. Future developments could focus on further enhancing peroxygenase activity and stability in organic solvents by using the CURE-UP screening platform, thereby reducing the required enzyme loading and enhancing overall curing efficiency. Additionally, the platform could be extended to other resin systems (*e.g.*, styrene-free polyester resins) to broaden its applicability and further reduce environmental impact.

Introduction

Unsaturated polyester resins (UPRs) are versatile thermosetting polymers widely used in the construction of storage tanks, boat hulls, wind turbine blades, and polymer concrete as reinforced and non-reinforced composite materials.[1] The mechanical strength of UPRs originates from the curing process, in which the polyester resin is cross-linked to form a solid polymer network (thermoset). Conventionally, styrene is used as a reactive diluent and acts as a cross-linking agent.[2] Cross-linking in UPR systems is initiated through the decomposition of organic peroxides (*e.g.*, methyl ethyl ketone peroxide; MEKP)[3] to generate radicals for the subsequent copolymerization of the cross-linking agent and UPR oligomer. To accelerate curing at room temperature, transition metal-based catalysts are often employed, with cobalt octoate being the most commonly used.[4] Recent health and environmental reports have raised serious concerns about the use of cobalt compounds, which might result in upcoming regulatory restrictions.[5–8] The latter has prompted the search for safer and more sustainable alternatives, such as iron-, vanadium-, manganese-, and copper-based accelerators.[5,9,10] Enzymes have not yet been considered as an alternative to cobalt accelerators for UPR systems.

Radical-generating enzymes are widely used as polymerisation initiators in applications such as hydrogel synthesis[11,12]

[a]*Institute of Biotechnology, RWTH Aachen University, Worringerweg 3, 52074 Aachen, Germany. E-mail: u.schwaneberg@biotec.rwth-aachen.de*
[b]*BYK-Chemie, GmbH, Abelstraße 45, 46483 Wesel, Germany*

or surface functionalisation.[13,14] Prominent enzyme classes comprise laccases, H_2O_2-producing oxidases, or peroxidases.[15–17] Unspecific peroxygenases (UPOs) have proven to be of high synthetic interest due to their broad catalytic versatility,[18,19] their efficient production in yeast expression systems such as *Pichia pastoris*,[20,21] and their compact structure, which often results in high process stability when compared to other oxygenating enzymes.[22] Peroxygenases can also perform single-electron transfer peroxidase reactions, enabling their use in free-radical polymerisations.[23,24] Among the few characterised UPOs, the recently discovered *Hsp*UPO derived from *Hypoxylon* sp. EC38 has promising stability and activity properties for industrial applications.[25]

The primary challenge in implementing enzyme-initiated curing systems in polyester resins is the need to operate in organic solvents, since the presence of water interferes with the curing process and compromises the final material properties.[26] Organic solvents like acetonitrile, tetrahydrofuran, hexane, methanol, or dimethyl sulfoxide (DMSO) can be utilized as carrier solvents to ensure efficient penetration of the enzyme into the polyester resin. DMSO is a promising water-miscible cosolvent, which is widely used in biocatalysis and has low toxicity.[27–30] Even though the industrial utilisation of DMSO is often limited by its high boiling point (189 °C), which complicates its removal, it remains an attractive solvent for curing composites that do not require subsequent extraction.[31] However, DMSO as a dipolar aprotic solvent can induce conformational changes in enzyme by replacing enzyme-bound water molecules, especially on the surface of the enzyme, reducing flexibility and activity.[32] Further, DMSO has been reported to block substrate access tunnels,[33] or to bind non-specifically within the substrate pocket close to the active site.[34] Activity profiles in DMSO environments differ widely between enzyme classes. Although some enzymes (*e.g.*, lipases[30]) retain significant residual activity (~40%) even in 60vol% DMSO, the unspecific peroxygenase *Hsp*UPO loses almost all of its peroxidase activity in only 5 vol% DMSO when using hydrogen peroxide as the oxidant substrate.[25] Protein engineering methodologies, such as directed evolution[35,36] or molecular dynamics simulations combined with machine learning,[37] have proven to be powerful approaches for enhancing the organic solvent tolerance of enzymes.

In the case of UPOs, an engineered *Aae*UPO for improved tolerance to DMSO and other organic cosolvents (up to 3-fold activity increase at 15 vol% DMSO) was reported.[38] Among other regions, beneficial substitutions in respect to DMSO tolerance were found in the enzyme's substrate tunnel.[38] Engineering of the substrate tunnel is a frequently applied strategy to improve catalytic performance of enzymes when using non-natural substrates or solvents. Successful engineering campaigns have been reported for various enzyme classes, including lipases,[39] dehalogenases,[33,40] and hydrolases.[41,42] Although substrate tunnel engineering of *Hsp*UPO has not yet been studied in detail, a competitive DMSO inhibition in the substrate tunnel by blockage of the catalytically active heme group was suggested.[25]

In most of the reported UPO engineering campaigns, high-throughput screening assays based on the mediator 2,2′-azino-bis(3-ethylbenzothiazoline-6-sulfonic acid) (ABTS) were employed.[38,43–46] Mediators are often implemented in enzymatic polymerisation processes to enhance the electron transfer between the enzyme and the monomer.[16,47,48] However, the ABTS mediator is not preferred for industrial use due to its high costs and comparably low performance.[49] As an alternative, naphtholic compounds, such as 2-nitroso-1-naphthol-4-sulfonic acid, have been reported as effective redox mediators, for example, in laccase-catalysed dye decolourisation.[50]

Key to a successful directed evolution campaign is a reliable assay system (*e.g.*, based on coupling reactions with chromophores) with a coefficient of variation (CV) below 15% in a 96-well microtiter plate (MTP) format.[51] Phenoxy- and naphthoxy-radicals have been reported as suitable substrates for quantification *via* the chromophore 4-aminoantipyrine (4-AAP).[52–54] Furthermore, 4-AAP has successfully been utilised in screening systems with CVs of around 10%.[55,56]

Raman spectroscopy is a non-invasive analytical technique that detects molecular vibrations and can be used for the identification and characterisation of chemical products, metabolites, and enzyme activities.[57,58] The lack of suitable instrumentations has hindered its use in directed evolution campaigns (*e.g.*, in 96-well MTP format).[58] Recent advancements in sensitivity, however, enable Raman spectroscopy in 96-well format, thereby expanding the potential application.[59] Raman spectroscopy has previously been applied to monitor the cross-linking of styrene in UPRs or related polymerisations.[60–62]

In this work, we report the first directed evolution platform for engineering unspecific peroxygenases to enhance curing of unsaturated polyester resins with a two-step screening system employing a 96-well Raman spectrometer. The mediator 6-hydroxy-2-naphthoic acid (6HNA) was confirmed as a substrate for *Hsp*UPO peroxidase activity, using MEKP (in its stabilised form Butanox® M-50) as the peroxide and 4-AAP for colourimetric quantification of enzymatic radical formation. Motivated by these findings, we developed and validated the two-step screening platform CURE-UP (**C**uring of **U**nsaturated polyester **RE**sin with **U**nspecific **P**eroxygenases). In the first step, CURE-UP identifies peroxygenase variants with improved DMSO tolerance, followed by measurment of their curing performance by Raman spectroscopy in 96-well microtiter plates, which is a first in enzyme engineering. The CURE-UP platform was validated by screening three site-saturation mutagenesis (SSM) libraries (in total 504 enzyme variants) under application-relevant conditions, yielding an improved *Hsp*UPO variant with respect to DMSO tolerance and unsaturated polyester resin curing performance.

Results and discussion

Principle of the CURE-UP screening platform

Fig. 1 summarises the two steps of the CURE-UP screening platform, in which *Hsp*UPO variants with improved DMSO tol-

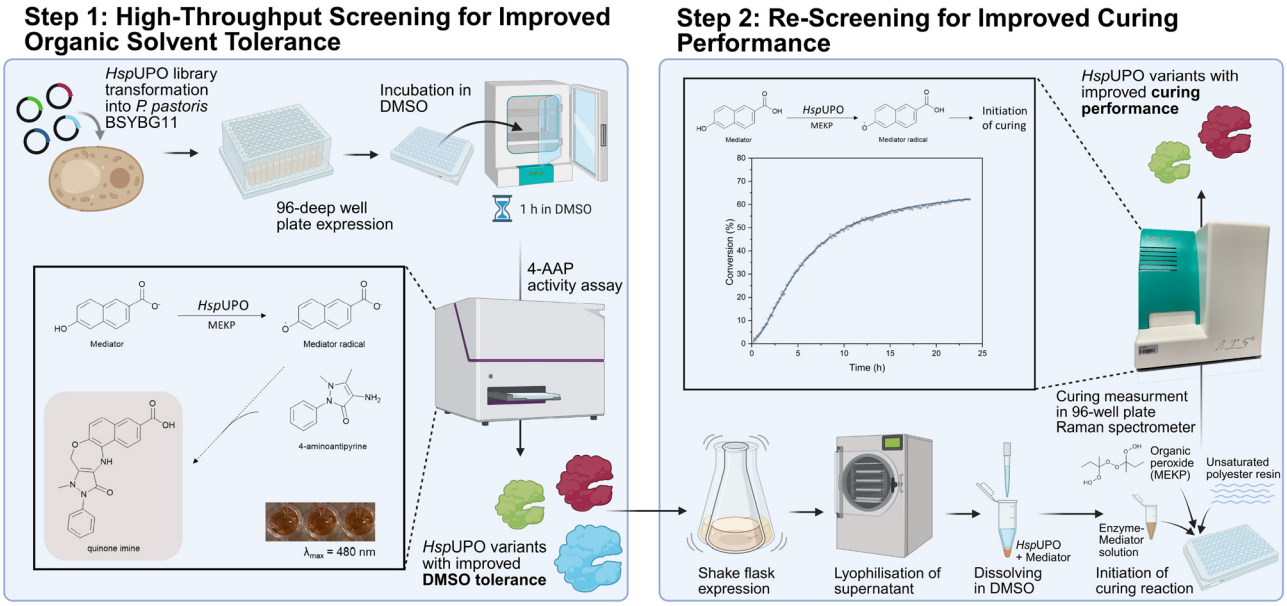

Fig. 1 Overview of the CURE-UP screening platform for the enzymatic curing of unsaturated polyester resins. Step 1: High-throughput screening for increased *Hsp*UPO tolerance to dimethyl sulfoxide (DMSO). Three site-saturation mutagenesis libraries of *Hsp*UPO were genomically integrated and expressed in *Pichia pastoris* BSYBG11 in 96-deep-well plates. Culture supernatants were incubated in 45 vol% DMSO, and mediator (6-hydroxy-2-naphthoic acid) radical formation was quantified *via* a 4-aminoantipyrine (4-AAP) based colorimetric assay. Methyl ethyl ketone peroxide (MEKP; Butanox® M-50) was used as the oxidant substrate. The 4-AAP reacts with the oxidised mediator, producing a red quinone imine chromophore (λ_{max} = 480 nm). Step 2: Re-screening of selected *Hsp*UPO variants to determine curing performance. Variants were expressed in 1 L shake flasks (200 mL cultures), lyophilised, and dissolved in DMSO together with the mediator. The viscous polyester resin was supplemented with the enzyme-mediator solution and the organic peroxide MEKP (Butanox® M-50). Curing was monitored in 96-well plates using Raman spectroscopy (AcuScan® 1500, AcuTech Scientific, USA), measuring the consumption of styrene vinyl groups at 1630 cm^{-1}. The expression of DMSO tolerant *Hsp*UPO variants in shaking flasks is necessary to obtain sufficient quantities of *Hsp*UPO for polyester resin curing under conditions close to application conditions. Created with BioRender.com.

erance are identified (Step 1) and their accelerator performance for polyester resin curing is determined (Step 2). DMSO tolerance was identified as a key limiting factor in *Hsp*UPO activity under application-relevant conditions (Fig. S1). The polyester resin curing was monitored with Raman spectroscopy by following the decrease of characteristic bands from styrene monomer vinyl double bonds at 1630 cm^{-1}. The radical mediator 6HNA was used in both steps of the screening system to ensure identification of *Hsp*UPO variants close to application conditions.

Establishment and validation of the high-throughput screening system to identify *Hsp*UPO variants with improved organic solvent tolerance (Step 1)

The 4-AAP assay is based on the coupling of 6HNA radicals, generated by *Hsp*UPO, with the chromophore 4-AAP, resulting in a red-coloured quinone imine (λ_{max} = 480 nm). Assay conditions were optimised for 96-well microtiter plates by varying concentrations of the mediator 6HNA, the chromophore 4-AAP, and the organic peroxide Butanox® M-50 (Fig. S2 and S3). A signal maximum was reached using 20 mM 6HNA, 2 mM 4-AAP, and 0.023 vol% Butanox® M-50 in the assay solution. Although *Hsp*UPO activity was not fully saturated at 20 mM 6HNA, higher concentrations could not be used due to solubility limitations in aqueous solutions. As selection criteria for improved *Hsp*UPO tolerance to DMSO, the activity ratio after 1 h incubation with and without 45 vol% DMSO was used. In the activity assay, samples were diluted by addition of an equal volume of assay solution, resulting in a final DMSO concentration of 27.5 vol%. Under these conditions, *Hsp*UPO retained approximately 30% residual activity, which is a suitable residual activity to identify improved variants.[63] The main advantage of measuring in the presence and absence of DMSO is the minimisation of differences resulting from expression levels, which commonly occur in directed evolution campaigns using *P. pastoris* strains with genomic integrated enzyme variant libraries.[64] After optimisation of all assay parameters, a true CV of 12% was obtained for the residual activity in DMSO (Fig. 2). CVs below 15% are routinely and successfully employed in traditional directed evolution campaigns.[51,55,65]

The use of the organic peroxide MEKP (Butanox® M-50) instead of hydrogen peroxide is an important prerequisite to be close to application conditions and to ensure the transferability between the screening steps. Using hydrogen peroxide, the activity of *Hsp*UPO wild type (WT) rapidly declined even at low DMSO concentrations, whereas with MEKP, enzyme activity is increased at low DMSO concentration (up to 15 vol%) and only diminished at significantly higher DMSO levels (Fig. S1; $IC_{50}(H_2O_2)$ = 6%, IC_{50}(MEKP) = 49%). Increases in activity above 100% are often reported for organic solvent

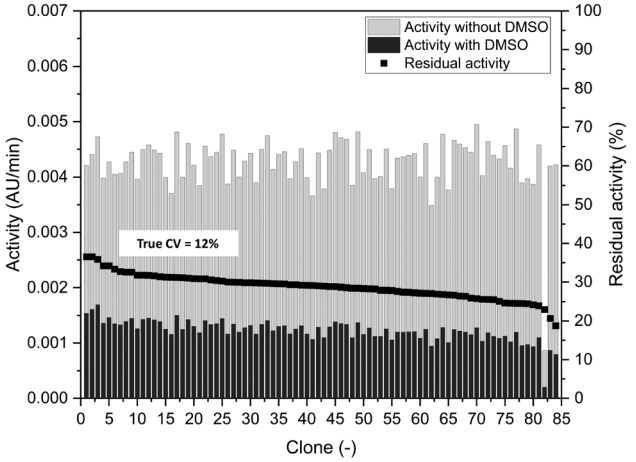

Fig. 2 True coefficient of variation (CV) of the developed colorimetric 4-aminoantipyrine (4-AAP) screening system to quantify *Hsp*UPO activity in mediator (6-hydroxy-2-napthoic acid) oxidation. Activity values (Absorbance units (AU) at 480 nm per minute) of *Hsp*UPO wild type in a 96-well microtiter plate were measured before and after 1 h incubation in 45 vol% DMSO. The graph shows *Hsp*UPO wild type activity before (light grey) and after DMSO incubation (black) with determined residual activity (black squares) to calculate the true coefficient of variation (CV; 12%).

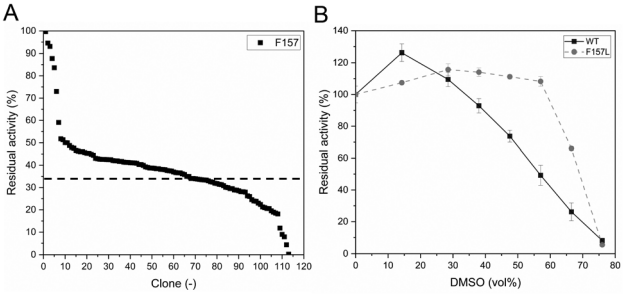

Fig. 3 Results of the site-saturation mutagenesis library screening of *Hsp*UPO F157. (A) Results of residual activity of *Hsp*UPO F157 site-saturation mutagenesis library. Residual activity was calculated from 4-AAP assay activity measurements before and after 1 h incubation in 45 vol% DMSO. 176 variants were screened in total; shown are only variants with measurable initial activity. Average of wild type residual activity is indicated as a dotted line. (B) DMSO residual activity of *Hsp*UPO wild type (WT, solid line) and the variant F157L (dashed line). Activities were determined after 1 h incubation in different concentrations (vol%) of DMSO *via* the 4-AAP assay. Data from at least two measurements are presented as mean ± SD.

studies with DMSO and have been attributed to DMSO adsorption on the enzyme surface (which reduces polar interactions within the enzyme), increasing flexibility and, therefore, activity.[66,67]

The CURE-UP screening platform was validated by screening three SSM libraries at the residues L61, F157, and L209 in the substrate tunnel of *Hsp*UPO.[25] Guided by visual inspection and CAVER analysis of the *Hsp*UPO crystal structure (PDB: 7O1R), residues were selected whose side chains define tunnel geometry, are located on three distinct α-helices forming the tunnel, and are distributed along the tunnel axis, avoiding clustering within a single region (Fig. S4 and Table S1).[68] For each saturated position, 168 variants were screened together with twelve WT and twelve empty vector controls, in the presence and absence of DMSO (in total 1152 screened wells).

Screening of the SSM libraries revealed that F157 has a significant influence on the DMSO tolerance of *Hsp*UPO (Fig. 3A), in contrast to positions L61 and L209 (Fig. S5). The five best performing clones were sequenced; interestingly, the substitution of phenylalanine to leucine occurred five times, using different codons (TTG, CTG, or CTT). The *Hsp*UPO F157L variant was subsequently characterised for its improved DMSO tolerance. While maintaining comparable activity values without DMSO (Fig. S6), F157L showed a 2.5-fold increased residual activity after incubation in 67 vol% DMSO compared to the WT enzyme (Fig. 3B; WT: 26.2 ± 3.9%, F157L: 66.1 ± 0.9%).

The obtained *Hsp*UPO variant F157L (in codons TTG, CTG, or CTT) demonstrates that the 4-AAP based screening system is robust and can efficiently identify *Hsp*UPO variants with improved DMSO tolerance.

Re-screening of the *Hsp*UPO F157L variant to determine improved curing performance under application conditions (Step 2)

Fig. 1 Step 2 illustrates the procedure used to evaluate the performance of *Hsp*UPO in unsaturated polyester resin curing. *P. pastoris* expression in shaking flasks was performed to produce *Hsp*UPO WT and its variant for Raman spectroscopy-based curing measurements in 96-well plate format (AcuScan® 1500, AcuTech Scientific, USA). All measurements were performed using lyophilised *Hsp*UPO-containing expression supernatant. Comparability of *Hsp*UPO content in the supernatant was ensured through protein normalisation *via* an automated protein electrophoresis system (2100 Bioanalyzer, Agilent Technologies, USA) prior to lyophilisation (Fig. S7).

The curing analysis was performed by monitoring the cross-linking of styrene monomers, initiated by *Hsp*UPO-catalysed formation of mediator radicals (Fig. 4A). In detail, the normalised Raman intensity of the C=C stretching vibration band at ν = 1630 cm^{-1} corresponds to the vinyl group of styrene monomer and decreases during polymerisation due to styrene consumption. The kinetics were monitored by calculating the ratio of the vinyl band to the carbonylic C=O stretching vibration at ν = 1730 cm^{-1} from the unsaturated polyester resin (Fig. 4B).[61] The slight decrease of Raman signals at ν = 1410 cm^{-1} (vinyl C–H band, styrene) and ν = 1600 cm^{-1} (aromatic C=C band, styrene) can likely be attributed to an expected styrene evaporation, and is also reflected in a small baseline drift in the no-enzyme negative control (Fig. S8).[61]

Fig. 5A shows that the curing process proceeds for 24 h with an expected sigmoidal conversion profile, reflecting a slow initiation phase and a diffusion-limited plateau.[69] Styrene conversion (%) was calculated from ratios of Raman signals at ν = 1630 cm^{-1} and ν = 1730 cm^{-1}. In general, increasing the amount of lyophilised *Hsp*UPO from 0.5 to 1 wt% led to a

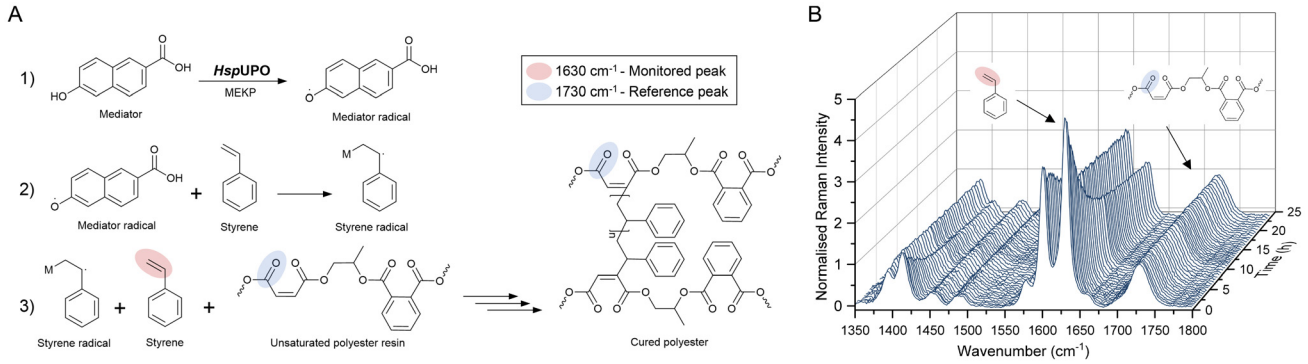

Fig. 4 Principle of unsaturated polyester resin curing analysis by Raman spectroscopy. (A) Proposed reaction scheme of *Hsp*UPO-catalysed radical formation of the mediator 6-hydroxy-2-naphthoic acid (1), followed by radical transfer to styrene monomer (2), initiating the styrene polymerisation and cross-linking reaction within the unsaturated polyester resin (3). The styrene vinyl group (ν = 1630 cm^{-1}, marked in red) polymerises, resulting in a signal decrease over time, whereas the carbonyl C═O group of the unsaturated polyester resin (ν = 1730 cm^{-1}, marked in blue) is used as reference. *Hsp*UPO = Unspecific peroxygenase from *Hypoxylon* sp. EC38; Mediator M = mediator (6-hydroxy-2-naphthoic acid); MEKP = methyl ethyl ketone peroxide (Butanox® M-50). (B) Change in the normalised Raman spectrum during 24 h of curing, initiated with 1 wt% of *Hsp*UPO WT-containing lyophilised supernatant and 0.5 vol% Butanox® M-50.

faster progression of curing and higher conversion after 24 h (Fig. 5A). A maximum conversion of 79% was achieved using 1 wt% *Hsp*UPO WT, while at least 0.75 wt% was required to surpass 50% conversion in 24 h.

To further assess the curing performance of the *Hsp*UPO WT and its variant, the data were fitted to a logistic function, and conversion rates were determined from its derivative (Fig. S9). A linear dependence of the maximum conversion rate on enzyme concentration was observed between 0.5 and 1 wt% lyophilised *Hsp*UPO WT (Fig. 5B; 4.26, 7.63, and 12.22% h^{-1} for 0.5, 0.75, and 1 wt%, respectively). Curing performance of *Hsp*UPO WT and variant F157L was determined with 0.75 wt% lyophilised supernatant. Variant F157L achieved a significantly higher conversion after 24 h than HspUPO WT (Fig. 5C; WT: 63.6 ± 0.3%, F157L: 66.5 ± 0.9%; p = 0.033). Most notably, F157L showed a 1.2-fold increase in maximum conversion rate compared to *Hsp*UPO WT (Fig. 5D; WT: 8.22 ± 0.09% h^{-1}, F157L: 10.14 ± 0.38% h^{-1}). Thereby, it is confirmed that screening for improved DMSO tolerance can yield *Hsp*UPO variants with improved polyester resin curing performance under conditions close to application conditions.

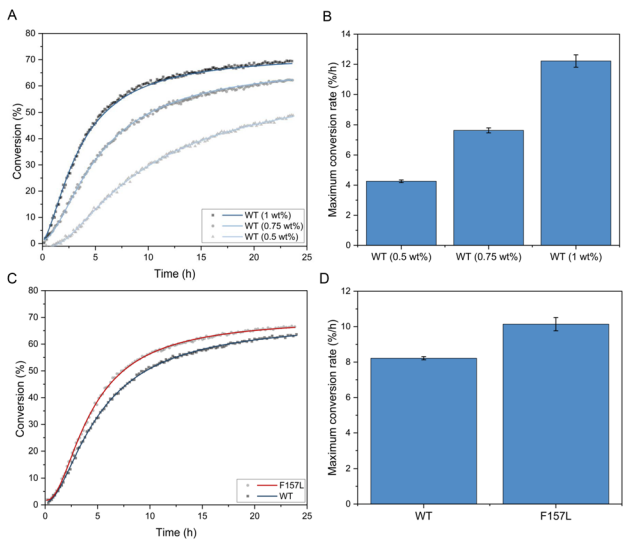

Fig. 5 Unsaturated polyester resin curing with *Hsp*UPO wild type (WT) and evolved variant F157L. (A) Curing measurements using varying amounts (wt% relative to the resin) of *Hsp*UPO WT-containing lyophilised supernatant. (B) Maximum conversion rates of the curing reaction initiated by varying amounts of *Hsp*UPO WT. Data from three measurements are presented as mean ± SEM. (C) Curing measurements for *Hsp*UPO WT and the improved variant F157L (0.75 wt% lyophilised supernatant). (D) Maximum conversion rates of the curing reaction initiated by *Hsp*UPO WT and variant F157L (0.75 wt% lyophilised supernatant). Data from three measurements are presented as mean ± SEM.

Previous studies have demonstrated that UPOs can be engineered for improved organic solvent tolerance, with beneficial substitutions frequently located in the substrate tunnel.[38] In line with these findings, the present work identified a tunnel substitution but extends earlier approaches by directly linking organic solvent tolerance engineering to curing performance in unsaturated polyester resins.

Conclusions

The two-step screening platform CURE-UP, developed for directed evolution of enzymes for the curing unsaturated polyester resins, has been successfully established and validated using the unspecific peroxygenase *Hsp*UPO. The *Hsp*UPO variant F157L has a 2.5-fold improved residual activity in DMSO and a 1.2-fold improved curing performance. The latter was monitored by Raman spectroscopy in a 96-well plate format, demonstrating the applicability of Raman spectroscopy as an analytical screening technology in directed evolution experiments. The CURE-UP screening platform is likely transferable to other polymerisation reactions, as long as the functional group being cross-linked is readily detectable by Raman

spectroscopy. In the long term, the CURE-UP screening platform can be utilised to enhance the curing performance of unspecific peroxygenases further, potentially enabling them to become an equivalent replacement for toxic cobalt accelerators.

Experimental section

Materials

All commercially available chemicals were purchased at analytical or higher grade from Merck (Darmstadt, Germany), New England Biolabs (Ipswich, USA), AppliChem (Darmstadt, Germany), Carl Roth (Karlsruhe, Germany), unless otherwise specified. Q5® High-Fidelity 2X Master Mix and SwaI restriction enzyme were purchased from New England Biolabs (Ipswich, USA). Dimethyl sulfoxide (analytical grade; AppliChem, Darmstadt, Germany), Butanox® M-50 (S u. K Hock GmbH, Regen, Germany), and Palatal p4-01 (AOC Deutschland GmbH, Kaiserslautern, Germany) were used.

Methods

Gene construction. The gene encoding *Hsp*UPO (Table S2) was cloned into the *P. pastoris* shuttle vector pBSY5S1Z (Bisy GmbH, Austria), containing the glucose-repressed and methanol-inducible P_{DF} promoter and an α-mating signal peptide for secretion.

Generation of site-saturation mutagenesis libraries. Site-Saturation Mutagenesis (SSM) libraries at positions L61, F157, and L209 were generated using NNK primers (Table S3). Polymerase chain reactions (PCR) were conducted using Q5 polymerase (New England Biolabs, USA). PCR products were transformed into electrocompetent *E. Cloni®* 10G cells (Biosearch Technologies, UK) and selected on LB Agar plates supplemented with 50 μg mL^{-1} Zeocin. Colonies were pooled for plasmid isolation, and the isolated plasmids linearized using SwaI restriction enzyme for genomic integration. Then, 300 ng μL^{-1} DNA was transformed into electro-competent *P. pastoris* BSYBG11 cells for expression. Positive transformants were selected on YPD Agar plates supplemented with 100 μg mL^{-1} Zeocin.

Library expression. Expression of SSM libraries was performed in 96-Deep well plates, covered with a breathable sealing film. Single colonies were inoculated into 250 μL buffered minimal dextrose (BMD1) medium (1.34 w/v% yeast nitrogen base without amino acids, 4×10^{-5} w/v% biotin, 200 mM potassium phosphate buffer, pH 6.0, and 1 w/v% glucose) and incubated for 36 h at 30 °C, 900 rpm, and 70% humidity. Expression was induced by adding 250 μL buffered minimal methanol (BMM2) medium (1.34 w/v% yeast nitrogen base without amino acids, 4×10^{-5} w/v% biotin, 200 mM potassium phosphate buffer, pH 6.0, and 1 vol% methanol). Expression was further induced by addition of 50 μL buffered minimal methanol (BMM10) medium (1.34 w/v% yeast nitrogen base without amino acids, 4×10^{-5} w/v% biotin, 200 mM potassium phosphate buffer, pH 6.0, and 5 vol% methanol) 8, 24, 48, 72, 96, and 120 h after first induction. The supernatant was separated from the cells by centrifugation (Eppendorf 5810R; 4 °C, 3220*g*, 15 min) and stored at 4 °C until screening.

High-throughput library screening. A 4-aminoantipyrine (4-AAP) based assay was used to screen for enzyme variants with improved DMSO tolerance. To determine the activity without DMSO, 20 μL culture supernatant were mixed with 80 μL screening buffer (200 mM Bis-Tris, pH 6.5) in a 96-well MTP. 100 μL 4-AAP assay solution (20 mM 6-hydroxy-2-naphtoic acid, 2 mM 4-AAP, 0.023 vol% Butanox® M-50, in screening buffer) were added to each well and shaken for 30 s at 1000 rpm. The resulting colour change was measured at 480 nm in an MTP-reader (CLARIOstar, BMG LABTECH, Ortenberg, Germany) for 10 min. To determine the activity with DMSO, 40 μL culture supernatant were transferred to a 96-well V-bottom MTP and mixed with 160 μL screening buffer containing 56.25 vol% DMSO, resulting in a final concentration of 45 vol%. To remove any precipitated salts, the MTPs were centrifuged (Eppendorf 5810R; RT, 3220*g*, 1 min) and 100μL were transferred to a new 96-well U-bottom MTP. After incubation for 1 h at room temperature, the activity was measured as described above, and residual activity was calculated using the following equation:

$$\text{Residual activity } (\%) = (\text{activity}_{\text{DMSO}}/\text{activity}_{\text{without DMSO}}) \times 100$$

Improved hits were sequenced by streaking them onto YPD agar plates, followed by colony PCR using Q5 polymerase (for primer sequences see Table S3). The PCR product was purified using a PCR clean-up kit (Macherey-Nagel GmbH & Co. KG, Germany) and sent for sequencing (Eurofins Genomics Germany GmbH, Germany).

Shake flask expression. Colonies were inoculated in 180 mL BMD1 medium in 1.5 L Ultra Yield™ flasks (Thomson Instrument Company, USA). After 60 h incubation (28 °C, 140 rpm), expression was induced by addition of 20 mL BMM10 medium. The expression was further induced by addition of 0.5 vol% Methanol 8, 24, 48, 72, 96, and 120 h after first induction. Cells were separated from culture supernatant by centrifugation (Eppendorf 5920 R, Eppendorf GmbH, Germany), and the supernatant was concentrated and desalted by ultrafiltration (Amicon® Ultra Centrifugal Filter, 10 kDa, Merck KGaA, Germany).

Purification of *Hsp*UPO. For purification, the culture supernatant was buffer-exchanged to purification buffer (20 mM Tris-Bis, pH 6.5) using PD-10 desalting columns (Cytiva, USA). Anion-exchange chromatography was performed using self-packed TOYOPEARL® SuperQ-650S resin (Tosoh Bioscience GmbH, Germany) operated under gravity flow. Bound proteins were eluted by stepwise increasing NaCl concentrations, and fractions exhibiting an appropriate Reinheitszahl (A_{420}/A_{280}) were pooled and buffer-exchanged into storage buffer (100 mM HEPES, pH 8.0). Protein concentrations were determined using the Bradford assay.

Residual enzyme activity determination. Residual enzyme activity was determined using a 4-AAP–based colorimetric

assay, as used for the screening experiments. In detail, 5 μL of purified enzyme stock solution (200 μg mL^{-1}) were mixed with 95 μL screening buffer containing different concentrations of DMSO in a 96-well MTP. After 1 h of incubation at room temperature, the reaction was initiated by addition of 100 μL 4-AAP assay solution, and the increase in absorbance at 480 nm was measured for 10 min. Enzyme activity was calculated from the initial linear slope of the absorbance change and reported as absorbance units per minute per microgram of protein (AU min^{-1} μg^{-1}). Residual activity was calculated as described above.

Raman spectroscopy-based re-screening for curing performance. Variants were re-screened for improved curing of unsaturated polyester resin using a 96-well Raman spectrometer. Therefore, *Hsp*UPO was expressed in shake flasks. The amount of recombinant protein was determined using the 2100 Bioanalyzer (14–230 kDa kit, Agilent, USA) and normalised by dilution with ddH_2O (600 μl final volume). Samples were frozen in liquid nitrogen and lyophilised overnight (approx. 18 h, Alpha 1-2 LDplus, Christ, Germany).

The enzyme-mediator solution was prepared by dissolving lyophilised *Hsp*UPO-containing supernatant (7.6 wt% for 1 wt% final concentration in the resin, *e.g.*), 6-hydroxy-2-naphthoic acid (29.5 wt%), and Triton X-100 (0.04 wt%) in DMSO. Samples were shaken for 1 h and incubated at room temperature for 18 h. The enzyme-mediator solution (13.25 wt%, 94.5 μL) was mixed with the unsaturated polyester resin (Palatal p4-01; 86.75 wt%, 710 μL). The curing reaction was initiated by adding 3.8 μL Butanox® M-50 (0.5 wt%). Samples were stirred with a pipette tip and distributed in a 96-well MTP (PP, Greiner AG, Austria) as triplicates (180 μL).

Raman spectra were recorded in a 96-well Raman spectrometer (AcuScan® 1500, AcuTech Scientific, USA) for 24 h using a 785 nm laser as the excitation source. Wavenumbers ranged from 200 and 2000 cm^{-1}. The spectra were baseline corrected using the ZhangFit[70] function in Python 3.8.10, and the styrene conversion (C) was calculated from the ratio (R) of peak intensities (I) at 1630 cm^{-1} to 1730 cm^{-1}, with $R = I_{1630\ cm^{-1}}/I_{1730\ cm^{-1}}$ and $C\ (\%) = (1 - R_t/R_0) \times 100$ (where R_t is the normalised intensity at time t and R_0 is the normalised intensity at time 0). Obtained conversion data were fitted using the five-parameter logistic (5PL) function in OriginPro 2022 (OriginLab, Version 9.9.0.220). The conversion rate (% h^{-1}) was determined by numerically calculating the first derivative of the fitted 5PL function using Origin's differentiation tool.

Computational tunnel analysis. The substrate tunnel of *Hsp*UPO was analysed using the CAVER 3.0.3 plugin implemented in PyMOL, based on the crystal structure of *Hsp*UPO (PDB ID: 7O1R). Tunnel calculations were initiated from the heme cofactor using a minimum probe radius of 1.1 Å, a shell depth of 6 Å, a shell radius of 14 Å, and a clustering threshold of 3.5. Tunnel centerline and lining residues were extracted and further analysed using a custom Python script to determine axial positions along the tunnel.

Author contributions

C. J.: conceptualisation, methodology, formal analysis, investigation, resources, data curation, writing – original draft, writing – review and editing, visualisation, project administration; F. C.: writing – review and editing, supervision; T. B.: validation, writing – review and editing; M. N.: supervision; L. K.: methodology, investigation; T. R.: project administration, funding acquisition; U. S.: resources, writing – review and editing, supervision, project administration, funding acquisition.

Conflicts of interest

There are no conflicts to declare.

Data availability

The data supporting this article have been included as part of the supplementary information (SI). See DOI: https://doi.org/10.1039/d5gc06576c.

Additional raw data supporting the study's findings are available from the corresponding author upon reasonable request.

Acknowledgements

This work was funded by the Bundesministerium für Bildung und Forschung (BMBF; Project BoostLab6.1 – EnzyPol, 031B1159B). We thank Anton Glieder (Bisy GmbH) for providing the enzyme and expression vector.

During the preparation of this manuscript, the authors used the ChatGPT language model (OpenAI) for light editing tasks such as grammar and spelling correction. All content was subsequently reviewed and edited by the authors, who take full responsibility for the integrity and accuracy of the final text.

References

1 M. I. Ul Haq, *Russ. J. Appl. Chem.*, 2007, **80**, 1256–1269.
2 J. L. Koenig and P. T. K. Shih, *J. Polym. Sci., Part A-2*, 1972, **10**, 721–740.
3 E. L. Rodriguez, *Polym. Eng. Sci.*, 1991, **31**, 1022–1028.
4 R. Guo, Y. Wang, Y. Qi, A. G. Talma and J. Zhang, *Macromol. Res.*, 2018, **26**, 680–689.
5 N. Simpson, K. Maaijen, Y. Roelofsen and R. Hage, *Catalysts*, 2019, **9**, 825.
6 L. Leyssens, B. Vinck, C. van der Straeten, F. Wuyts and L. Maes, *Toxicology*, 2017, **387**, 43–56.
7 M. Behl, M. D. Stout, R. A. Herbert, J. A. Dill, G. L. Baker, B. K. Hayden, J. H. Roycroft, J. R. Bucher and M. J. Hooth, *Toxicology*, 2015, **333**, 195–205.

8 National Toxicology Program, Cobalt-Related Exposures. In: Program NT, editor. 15th Report on Carcinogens [Internet]: National Toxicology Program, 2021.
9 D. Rubeš, J. Vinklárek, L. Prokůpek, Š. Podzimek and J. Honzíček, *J. Mater. Sci.*, 2023, **58**, 6203–6219.
10 J. F. Jansen, I. Hilker, E. Kleuskens, G. Hensen, I. Kraeger and W. Posthumus, *Macromol. Symp.*, 2013, **329**, 142–149.
11 T. Su, D. Zhang, Z. Tang, Q. Wu and Q. Wang, *Chem. Commun.*, 2013, **49**, 8033–8035.
12 L. M. Johnson, B. D. Fairbanks, K. S. Anseth and C. N. Bowman, *Biomacromolecules*, 2009, **10**, 3114–3121.
13 H. Fukushima, M. Kohri, T. Kojima, T. Taniguchi, K. Saito and T. Nakahira, *Polym. Chem.*, 2012, **3**, 1123–1125.
14 C. Nenninger, F. Contreras, M. Vorobii, M. Sária Pereira de Passos, J. Gebauer, M. Nöth, L. Stütgens, H. El Kadaoui, T. Bergs and U. Schwaneberg, *Surf. Interfaces*, 2025, **60**, 106046.
15 W. Zhang and F. Hollmann, *Enzymatic Polymerization towards Green Polymer Chemistry*, 2019, pp. 343–356.
16 S. Zavada, T. Battsengel and T. F. Scott, *Int. J. Mol. Sci.*, 2016, **17**, 2110.
17 F. Hollmann and I. W. C. E. Arends, *Polymers*, 2012, **4**, 759–793.
18 A. Beltrán-Nogal, I. Sánchez-Moreno, D. Méndez-Sánchez, P. Gómez de Santos, F. Hollmann and M. Alcalde, *Curr. Opin. Struct. Biol.*, 2022, **73**, 102342.
19 Y. Wang, D. Lan, R. Durrani and F. Hollmann, *Curr. Opin. Chem. Biol.*, 2017, **37**, 1–9.
20 S. Bormann, H. Kellner, J. Hermes, R. Herzog, R. Ullrich, C. Liers, R. Ulber, M. Hofrichter and D. Holtmann, *Antioxidants*, 2022, **11**, 223.
21 K. Ebner, L. Pfeifenberger, C. Rinnofner, V. Schusterbauer, A. Glieder and M. Winkler, *Catalysts*, 2023, **13**, 206.
22 P. Molina-Espeja, M. Cañellas, F. J. Plou, M. Hofrichter, F. Lucas, V. Guallar and M. Alcalde, *ChemBioChem*, 2016, **17**, 341–349.
23 M. Hofrichter and R. Ullrich, *Curr. Opin. Chem. Biol.*, 2014, **19**, 116–125.
24 S. Peter, *Oxyfunctionalization of alkanes, alkenes and alkynes byunspecific peroxygenase (EC 1.11.2.1)*, PhD thesis, TU Dresden, Dresden, Germany, 2013.
25 L. Rotilio, A. Swoboda, K. Ebner, C. Rinnofner, A. Glieder, W. Kroutil and A. Mattevi, *ACS Catal.*, 2021, **11**, 11511–11525.
26 S.-B. Lee, T. J. Rockett and R. D. Hoffman, *Polymer*, 1992, **33**, 3691–3697.
27 J. T. Chin, S. L. Wheeler and A. M. Klibanov, *Biotechnol. Bioeng.*, 1994, **44**, 140–145.
28 C.-N. Wang, S. Qiu, F.-F. Fan, C.-J. Lyu, S. Hu, W.-R. Zhao, J.-Q. Mei, L.-H. Mei and J. Huang, *Biotechnol. J.*, 2023, **18**, e2300120.
29 J. E. Willson, D. E. Brown and E. K. Timmens, *Toxicol. Appl. Pharmacol.*, 1965, **7**, 104–112.
30 M. Z. Kamal, P. Yedavalli, M. V. Deshmukh and N. M. Rao, *Protein Sci.*, 2013, **22**, 904–915.
31 M. Martí, L. Molina, C. Alemán and E. Armelin, *ACS Sustainable Chem. Eng.*, 2013, **1**, 1609–1618.
32 H. Cui, L. Zhang, L. Eltoukhy, Q. Jiang, S. K. Korkunç, K.-E. Jaeger, U. Schwaneberg and M. D. Davari, *ACS Catal.*, 2020, **10**, 14847–14856.
33 T. Koudelakova, R. Chaloupkova, J. Brezovsky, Z. Prokop, E. Sebestova, M. Hesseler, M. Khabiri, M. Plevaka, D. Kulik, I. Kuta Smatanova, P. Rezacova, R. Ettrich, U. T. Bornscheuer and J. Damborsky, *Angew. Chem.*, 2013, **125**, 2013–2017.
34 N. Milčić, V. Stepanić, I. Crnolatac, Z. Findrik Blažević, Z. Brkljača and M. Majerić Elenkov, *Chem. – Eur. J.*, 2022, **28**, e202201923.
35 F. Arnold, *Trends Biotechnol.*, 1990, **8**, 244–249.
36 H. Cui, T. H. J. Stadtmüller, Q. Jiang, K.-E. Jaeger, U. Schwaneberg and M. D. Davari, *ChemCatChem*, 2020, **12**, 4073–4083.
37 R. Ma, Y. Li, M. Zhang and F. Xu, *Syst. Microbiol. Biomanuf.*, 2023, **3**, 427–439.
38 J. Martin-Diaz, P. Molina-Espeja, M. Hofrichter, F. Hollmann and M. Alcalde, *Biotechnol. Bioeng.*, 2021, **118**, 3002–3014.
39 S. Gihaz, M. Kanteev, Y. Pazy and A. Fishman, *Appl. Environ. Microbiol.*, 2018, **84**, e02143–e02118.
40 J. Brezovsky, P. Bábková, O. Degtjarik, A. Fořtová, A. Góra, I. Iermak, P. Řezáčová, P. Dvořák, I. Smatanová, Z. Prokop, R. Chaloupkova and J. Damborský, *ACS Catal.*, 2016, **6**, 7597–7610.
41 X.-D. Kong, S. Yuan, L. Li, S. Chen, J.-H. Xu and J. Zhou, *Proc. Natl. Acad. Sci. U. S. A.*, 2014, **111**, 15717–15722.
42 A. G. Hamre, E. Ebbestad Frøberg, V. Eijsink and M. Sørlie, *Arch. Biochem. Biophys.*, 2017, **620**, 35–42.
43 J. Martin-Diaz, C. Paret, E. García-Ruiz, P. Molina-Espeja and M. Alcalde, *Appl. Environ. Microbiol.*, 2018, **84**, e00808–e00818.
44 D. M. Mate, M. A. Palomino, P. Molina-Espeja, J. Martin-Diaz and M. Alcalde, *Protein Eng., Des. Sel.*, 2017, **30**, 189–196.
45 P. Molina-Espeja, E. Garcia-Ruiz, D. Gonzalez-Perez, R. Ullrich, M. Hofrichter and M. Alcalde, *Appl. Environ. Microbiol.*, 2014, **80**, 3496–3507.
46 X. Yan, X. Zhang, H. Li, D. Deng, Z. Guo, L. Kang and A. Li, *JACS Au*, 2024, **4**, 1654–1663.
47 S. Tanahashi, B. Xie, Y. Teramoto and T. Takano, *J. Wood Sci.*, 2024, **70**, 1–9.
48 K. Won, Y. H. Kim, E. S. An, Y. S. Lee and B. K. Song, *Biomacromolecules*, 2004, **5**, 1–4.
49 K. Zhang, Y. Wu, J. Huang and Y. Liu, *J. Chem.*, 2019, **2019**, 1–12.
50 S. Camarero, D. Ibarra, M. J. Martínez and A. T. Martínez, *Appl. Environ. Microbiol.*, 2005, **71**, 1775–1784.
51 O. Salazar and L. Sun, Evaluating a screen and analysis of mutant libraries, in *Directed Enzyme Evolution*, ed. F. H. Arnold, Humana Press, Totowa, NJ, 2003, pp. 85–97.
52 O. Otim, *Can. J. Chem.*, 2023, **101**, 364–376.

53 J. Kolšek, M. Perpar and V. Raznožnik, *Z. Anal. Chem.*, 1961, **183**, 119–123.
54 V. Vojinović, A. Azevedo, V. Martins, J. Cabral, T. Gibson and L. Fonseca, *J. Mol. Catal. B: Enzym.*, 2004, **28**, 129–135.
55 N. Lülsdorf, L. Vojcic, H. Hellmuth, T. T. Weber, N. Mußmann, R. Martinez and U. Schwaneberg, *Appl. Microbiol. Biotechnol.*, 2015, **99**, 5237–5246.
56 T. S. Wong, N. Wu, D. Roccatano, M. Zacharias and U. Schwaneberg, *J. Biomol. Screening*, 2005, **10**, 246–252.
57 R. S. Das and Y. K. Agrawal, *Vib. Spectrosc.*, 2011, **57**, 163–176.
58 B. D. Moore, L. Stevenson, A. Watt, S. Flitsch, N. J. Turner, C. Cassidy and D. Graham, *Nat. Biotechnol.*, 2004, **22**, 1133–1138.
59 H. Kawagoe, J. Ando, M. Asanuma, K. Dodo, T. Miyano, H. Ueda, M. Sodeoka and K. Fujita, *Sci. Rep.*, 2021, **11**, 15742.
60 S. Parnell, K. Min and M. Cakmak, *Polymer*, 2003, **44**, 5137–5144.
61 M. Skrifvars, P. Niemelä, R. Koskinen and O. Hormi, *J. Appl. Polym. Sci.*, 2004, **93**, 1285–1292.
62 J. C. Cruz and T. A. Osswald, *Polym. Eng. Sci.*, 2009, **49**, 2099–2108.
63 P. Yedavalli and N. M. Rao, *Protein Eng., Des. Sel.*, 2013, **26**, 317–324.
64 Z. Liu, B. Pscheidt, M. Avi, R. Gaisberger, F. S. Hartner, C. Schuster, W. Skranc, K. Gruber and A. Glieder, *ChemBioChem*, 2008, **9**, 58–61.
65 *Directed Enzyme Evolution: Screening and Selection Methods*, ed. F. H. Arnold, Methods in molecular biology, Humana Press, Totowa, NJ, 2003, vol. 230.
66 T. S. Wong, F. H. Arnold and U. Schwaneberg, *Biotechnol. Bioeng.*, 2004, **85**, 351–358.
67 E. Vignali, F. Tonin, L. Pollegioni and E. Rosini, *Appl. Microbiol. Biotechnol.*, 2018, **102**, 10579–10588.
68 E. Chovancova, A. Pavelka, P. Benes, O. Strnad, J. Brezovsky, B. Kozlikova, A. Gora, V. Sustr, M. Klvana, P. Medek, L. Biedermannova, J. Sochor and J. Damborsky, *PLoS Comput. Biol.*, 2012, **8**, e1002708.
69 B. Janković, *Chem. Eng. J.*, 2010, **162**, 331–340.
70 Z.-M. Zhang, S. Chen and Y.-Z. Liang, *Analyst*, 2010, **135**, 1138–1146.